Int. J. Heat Mass Transfer. Vol. 18, pp. 1473–1479. Pergamon Press 1975. Printed in Great Britain

NATURAL CONVECTION ABOVE A LINE HEAT SOURCE: HIGHER-ORDER EFFECTS AND STABILITY

C. A. HIEBER
Sibley School of Mechanical and Aerospace Engineering, Cornell University, Ithaca, NY 14853, U.S.A.

and

E. J. NASH
Department of Mechanical and Industrial Engineering, Clarkson College of Technology, Potsdam, NY 13676, U.S.A.

(*Received* 21 *February* 1975)

Abstract—The natural-convection plume above a horizontal line heat source is analyzed in terms of higher-order boundary-layer theory. A stability analysis of the resulting base flow is then performed by means of a systematic expansion for the disturbance field. Comparison of the theory with existing experimental results is found to be inconclusive.

NOMENCLATURE

a, radius of source;
b_1, numerical constant appearing in (2.1)–(2.2);
c, $\equiv \Omega/\alpha$;
g, gravitational acceleration (directed along negative x-axis);
G, $\equiv (x/\lambda)^{3/5} \equiv U\delta/\nu \equiv 1/\varepsilon$;
Gr, Grashof number of heat source, $\equiv g\beta(T_w - T_\infty)a^3/\nu^2$;
k, thermal conductivity of fluid;
Q, strength of heat source [W/m];
r, radial coordinate measured from center of source;
t, time;
T, temperature;
T_w, temperature of source;
T_∞, ambient fluid temperature;
u, x-component of velocity;
U, characteristic vertical velocity in plume, $\equiv (\nu/\lambda)(x/\lambda)^{1/5}$;
v, y-component of velocity;
x, vertical coordinate measured from center of source;
y, horizontal coordinate measured from center of source.

Greek symbols

α, $\equiv \delta(d\Lambda/dx)$;
β, coefficient of thermal expansion;
γ, $\equiv \Omega(d\alpha_1/d\Omega)$;
δ, characteristic thickness of plume, $\equiv \lambda(x/\lambda)^{2/5}$;
ΔT, characteristic temperature difference across plume, $\equiv \tilde{\Delta T}(\lambda/x)^{3/5}$;
$\tilde{\Delta T}$, $\equiv Q/k$;
ε, $\equiv \delta/x \equiv (\lambda/x)^{3/5}$;
ζ, vorticity;
η, similarity variable, $\equiv y/\delta$;
θ, defined in (3.1);
λ, $\equiv (\nu^2/(g\beta\Delta T))^{1/3}$;
Λ, defined in (3.1);
μ, angular polar coordinate measured from positive x-axis;
ν, kinematic viscosity;
σ, Prandtl number;
ϕ, defined in (3.1);
Ψ, streamfunction;
ω, frequency of disturbance;
Ω, $\equiv \omega\delta/U$.

1. INTRODUCTION

THE CLASSIC problem of laminar, natural-convection flow above a horizontal line heat source has received considerable attention in recent years ([1]–[7]) and has also been the "source" of some controversy.

In this paper, the zeroth-order plume structure of earlier investigations is extended (Section 2) to include: (i) the first-order correction arising from an interaction between the plume and the irrotational flow outside; (ii) the second-order correction (determinate to within a multiplicative constant) associated with a virtual displacement of the heat source. The stability of the laminar flow is then investigated (Section 3) by means of a systematic expansion which enables incorporating the effects of (i) above, together with other comparable effects which have been omitted in previous investigations. Discussion and comparison with earlier work is given in Section 4.

2. BOUNDARY-LAYER EXPANSION

In a manner completely analogous to that in [8], it can be shown that the leading-order terms for the streamfunction and temperature in the region

$$y = O(\delta), \quad x > O(\lambda)$$

are given by

$$\Psi = U\delta\{F_0(\eta) + \varepsilon F_1(\eta) + \varepsilon^{5/3} b_1 \Phi_1(\eta) + O(\varepsilon^2)\} \qquad (2.1)$$

$$T = T_\infty + \Delta T\{H_0(\eta) + \varepsilon H_1(\eta) + \varepsilon^{5/3} b_1 \Theta_1(\eta) + O(\varepsilon^2)\} \quad (2.2)$$

where the governing equations for F_0 and H_0 are given by

$$\left.\begin{aligned} &F_0''' + \tfrac{3}{5}F_0F_0'' - \tfrac{1}{5}F_0'F_0' = -H_0 \\ &H_0' + \tfrac{3}{5}\sigma F_0 H_0 = 0 \\ &F_0(0) = 0 = F_0''(0) = F_0'(\infty), \qquad \int_0^\infty F_0' H_0 \, d\eta = \frac{1}{2\sigma} \end{aligned}\right\} \quad (2.3)$$

and F_1 and H_1 are governed by:*

$$\left.\begin{aligned} &F_1''' + \tfrac{3}{5}F_0F_1'' + \tfrac{1}{5}F_0'F_1 = -H_1 \\ &H_1'' + \tfrac{3}{5}\sigma F_0 H_1' + \tfrac{6}{5}\sigma F_0' H_1 = -\tfrac{3}{5}\sigma F_1' H_0 \\ &F_1(0) = 0 = F_1''(0) = H_1'(0) = H_1(\infty), \qquad F_1'(\infty) = \kappa A_0 \end{aligned}\right\} \quad (2.4)$$

where

$$A_0 \equiv F_0(\infty), \quad \kappa \equiv \tfrac{3}{5}\cot\frac{2\pi}{5}. \quad (2.5)$$

In addition,

$$\Phi_1 = \tfrac{2}{5}\eta F_0' - \tfrac{3}{5}F_0, \quad \Theta_1 = \tfrac{2}{5}\eta H_0' + \tfrac{3}{5}H_0. \quad (2.6)$$

That is, F_0 and H_0 are driven by the integral condition in (2.3), which is a non-dimensional representation of the fact that the heat dissipated by the line source gets convected entirely by the plume. On the other hand, F_1 and H_1 arise from the inhomogeneous condition in (2.4) which represents a matching with the leading-order vertical velocity component of the irrotational flow outside, described by

$$\Psi \sim A_0 \nu \left(\frac{r}{\lambda}\right)^{3/5} \frac{\sin\frac{3}{5}(\pi-\mu)}{\sin\frac{3}{5}\pi}, \quad 0 < \mu < 2\pi, \; r > 0(\lambda). \quad (2.7)$$

This latter result, in turn, is driven by the influx velocity associated with F_0. Lastly, following Stewartson [9], Φ_1 and Θ_1 form the leading eigenfunction associated with the present boundary-layer expansion and can be interpreted physically as representing an apparent shift in the location of the heat source (to $x = b_1\lambda$: see Section 4) as seen by the plume region.

Numerical integration of the above for $\sigma = 0{\cdot}70$ gives the following values:

$$\left.\begin{aligned} &F_0'(0) = 0{\cdot}93273, \; H_0(0) = 0{\cdot}49654, \; F_0(\infty) = 2{\cdot}21121 \\ &F_1'(0) = 0{\cdot}09969, \; H_1(0) = -0{\cdot}25111 \\ &F_1(\eta) \sim \kappa A_0 \eta - 0{\cdot}38089 \quad \text{as} \quad \eta \to \infty. \end{aligned}\right\} \quad (2.8)$$

In particular, unlike the isothermal vertical-plate case, H_1 is non-zero. Indeed, this is necessary since the global energy-rate balance requires that

$$\int_0^\infty (F_0' H_1 + F_1' H_0)\, d\eta = 0, \quad (2.9)$$

which can be shown to be automatically satisfied by the solution of (2.4).

*It has been brought to the authors' attention by H. Shaukatullah of Cornell University that the problem for F_1 and H_1 has recently been solved by N. Riley, *Z. Angew. Math. Phys.* **25**, 817–828 (1974).

3. STABILITY ANALYSIS

Following a standard procedure in linear stability theory (see Lin [10]), we superimpose upon the above "base" flow an arbitrarily small disturbance of the form:

$$\left.\begin{aligned} \tilde\Psi &= U\delta\phi(\eta)\, e^{i(\Lambda(x)-\omega t)} + \text{c.c.} \\ \tilde T &= \Delta T \theta(\eta)\, e^{i(\Lambda(x)-\omega t)} + \text{c.c.} \end{aligned}\right\} \quad (3.1)$$

where "c.c." denotes "complex conjugate" and ϕ, θ and Λ are complex whereas the frequency, ω, is assumed to be real. Since the base flow is known in terms of an expansion in ε, it is appropriate to express the disturbance quantities in a similar manner, namely:

$$\begin{aligned} \phi &= \phi_1(\eta) + \varepsilon\phi_2(\eta) + \ldots \\ \theta &= \theta_1(\eta) + \varepsilon\theta_2(\eta) + \ldots \\ \Lambda &= \Lambda_1(x) + \varepsilon\Lambda_2(x) + \ldots \end{aligned} \quad (3.2)$$

whereas ω will be assumed given (i.e. consideration is being given to the response of the steady laminar flow to perturbations of various prescribed frequency). Additional quantities which will be employed below are the non-dimensional frequency, complex wavenumber and complex wavespeed, given respectively by:

$$\Omega \equiv \frac{\delta\omega}{U}, \quad (3.3)$$

$$\alpha \equiv \delta\frac{d\Lambda}{dx} = \alpha_1 + \varepsilon\alpha_2 + \ldots, \quad (3.4)$$

$$c \equiv \frac{\Omega}{\alpha} = c_1 + \varepsilon c_2 + \ldots. \quad (3.5)$$

The vorticity and energy equations, linearized in terms of disturbance quantities, are given by:

$$\left.\begin{aligned} &\frac{\partial\tilde\zeta}{\partial t} + \bar u\frac{\partial\tilde\zeta}{\partial x} + \tilde u\frac{\partial\bar\zeta}{\partial x} + \bar v\frac{\partial\tilde\zeta}{\partial y} + \tilde v\frac{\partial\bar\zeta}{\partial y} \\ &\qquad = \nu\left(\frac{\partial^2}{\partial y^2} + \frac{\partial^2}{\partial x^2}\right)\tilde\zeta - g\beta\frac{\partial\tilde T}{\partial y}, \end{aligned}\right\} \quad (3.6)$$

$$\left.\begin{aligned} &\frac{\partial\tilde T}{\partial t} + \bar u\frac{\partial\tilde T}{\partial x} + \tilde u\frac{\partial\bar T}{\partial x} + \bar v\frac{\partial\tilde T}{\partial y} + \tilde v\frac{\partial\bar T}{\partial y} \\ &\qquad = \frac{\nu}{\sigma}\left(\frac{\partial^2}{\partial y^2} + \frac{\partial^2}{\partial x^2}\right)\tilde T \end{aligned}\right\} \quad (3.7)$$

where the bar denotes the base-flow quantities of Section 2. In particular,

$$\tilde u = \frac{\partial\tilde\Psi}{\partial y} = U(\phi_1' + \varepsilon\phi_2' + \ldots)e^{i(\Lambda-\omega t)} + \text{c.c.} \quad (3.8)$$

$$\begin{aligned} \tilde v &= -\frac{\partial\tilde\Psi}{\partial x} \\ &= U\{-i\alpha_1\phi_1 + \varepsilon(\tfrac{2}{5}\eta\phi_1' - \tfrac{3}{5}\phi_1 - i\alpha_2\phi_1 \\ &\qquad - i\alpha_1\phi_2) + \ldots\}e^{i(\Lambda-\omega t)} + \text{c.c.} \end{aligned} \quad (3.9)$$

$$\begin{aligned} \tilde\zeta &= \frac{\partial\tilde v}{\partial x} - \frac{\partial\tilde u}{\partial y} \\ &= \frac{U}{\varepsilon x}\{(\alpha_1^2\phi_1 - \phi_1'') + \varepsilon(\tfrac{4}{5}i\alpha_1\eta\phi_1' - \tfrac{4}{5}i\alpha_1\phi_1 + 2\alpha_1\alpha_2\phi_1 \\ &\qquad + \alpha_1^2\phi_2 - \tfrac{1}{5}i\gamma\phi_1 - \phi_2'') + \ldots\}e^{i(\Lambda-\omega t)} + \text{c.c.} \end{aligned} \quad (3.10)$$

where

$$\gamma \equiv \Omega\frac{d\alpha_1}{d\Omega} \quad (3.11)$$

arises from $\partial\alpha_1/\partial x$ and the property that α_1 depends only upon Ω, being the eigenvalue of the inviscid problem [defined by equations (3.13) and (3.18) below]; i.e.

$$\frac{\partial\alpha_1}{\partial x}=\frac{\mathrm{d}\alpha_1}{\mathrm{d}\Omega}\frac{\partial\Omega}{\partial x}=\frac{\mathrm{d}\alpha_1}{\mathrm{d}\Omega}\frac{1}{5}\frac{\Omega}{x}\equiv\frac{\gamma}{5x}, \tag{3.12}$$

Ω being proportional to $x^{1/5}$ for fixed ω.

Carrying out the operations in (3.6) and ordering terms in powers of ε results in the following equations for the leading and next-order groupings {of order $U^2\,\phi/\delta^2$ and $\varepsilon U^2\,\phi/\delta^2$, respectively}:

$$L(\phi_1)\equiv i\alpha_1(F_0'-c_1)(\phi_1''-\alpha_1^2\phi_1)-i\alpha_1F_0'''\phi_1=0 \tag{3.13}$$

and

$$L(\phi_2)=\mathscr{F}_1+\alpha_2\mathscr{F}_2 \tag{3.14}$$

where

$$\begin{aligned}\mathscr{F}_1=\;&\phi_1''''-2\alpha_1^2\phi_1''+\alpha_1^4\phi_1+\theta_1'\\&-i\alpha_1F_1'(\phi_1''-\alpha_1^2\phi_1)+i\alpha_1F_1'''\phi_1\\&-\tfrac{4}{5}\alpha_1^2\eta F_0\phi_1'+\tfrac{3}{5}\alpha_1^2F_0\phi_1+\tfrac{3}{5}\alpha_1\gamma F_0'\phi_1+\tfrac{1}{5}F_0'\phi_1''\\&+\tfrac{1}{5}\phi_1'F_0''-\tfrac{3}{5}\alpha_1^2F_0\phi_1'+\tfrac{3}{5}F_0\phi_1'''\\&+\tfrac{3}{5}F_0'''\phi_1+c_1(\tfrac{4}{5}\alpha_1^2\eta\phi_1'-\tfrac{4}{5}\alpha_1^2\phi_1-\tfrac{1}{5}\alpha_1\gamma\phi_1),\end{aligned} \tag{3.15}$$

$$\mathscr{F}_2=-2i\alpha_1^2c_1\phi_1+3i\alpha_1^2F_0'\phi_1-iF_0'\phi_1''+iF_0'''\phi_1 \tag{3.16}$$

and, from the leading terms in (3.7),

$$\theta_1=H_0'\phi_1/(F_0'-c_1) \tag{3.17}$$

Appropriate conditions on the above are that the disturbances vanish at the edge of the plume and that $\tilde{u}$ be asymmetric with respect to the centerline, this mode having been found to be less stable than the symmetric case (see Pera and Gebhart [5]). Hence,

$$\phi_j'(0)=0=\phi_j(\infty),\ \text{all } j. \tag{3.18}$$

Since the homogeneous problem for ϕ_2 is identical to that for ϕ_1, it is required that

$$\int_0^\infty(\mathscr{F}_1+\alpha_2\mathscr{F}_2)\chi\,\mathrm{d}\eta=0 \tag{3.19}$$

where χ is a non-trivial solution of the adjoint homogeneous problem:

$$\left.\begin{aligned}&(F_0'-c_1)(\chi''-\alpha_1^2\chi)+2F_0''\chi'=0\\&\chi'(0)=0=\chi(\infty).\end{aligned}\right\} \tag{3.20}$$

Hence, the procedure for determining α_1 and α_2 is as follows. For a given Ω, equations (3.13) and (3.18) are solved for α_1 and $\phi_1(\eta)$ [note: $c_1=\Omega/\alpha_1$]. With α_1 known, χ is determined from (3.20). In addition, ϕ_1''' and ϕ_1'''' are obtained by successive differentiation of (3.13) whereas θ_1' is similarly derived from (3.17). Lastly, γ is obtained from knowing $\alpha_1(\Omega)$ at neighboring values of Ω, namely,

$$\gamma\simeq\Omega\frac{\alpha_1(\Omega+\Delta\Omega)-\alpha_1(\Omega-\Delta\Omega)}{2\Delta\Omega} \tag{3.21}$$

where $\Delta\Omega$ has been taken to be 0·02 in the results below. Hence, with χ, F_1 and F_2 known, α_2 is obtained from (3.19); i.e.

$$\alpha_2=-\int_0^\infty\mathscr{F}_1\chi\,\mathrm{d}\eta\Big/\int_0^\infty\mathscr{F}_2\chi\,\mathrm{d}\eta. \tag{3.22}$$

Again limiting attention to $\sigma=0{\cdot}70$, resulting values of α_1 and α_2 at various Ω are shown in Table 1. Based upon these values, the neutral-stability and amplification contours can be constructed. These are shown later in Section 4.

Table 1. Values of α_1, α_2 and $-\alpha_{2i}/\alpha_{1i}$ vs Ω

Ω	α_1	α_2	$-\alpha_{2i}/\alpha_{1i}$
0·02	0·0609 − 0·0580i	−0·033 + 0·779i	13·42
0·04	0·1150 − 0·0884i	−0·078 + 0·813i	9·20
0·06	0·1693 − 0·1069i	−0·123 + 0·842i	7·88
0·08	0·2213 − 0·1158i	−0·165 + 0·856i	7·40
0·10	0·2693 − 0·1181i	−0·198 + 0·860i	7·26
0·12	0·3130 − 0·1162i	−0·223 + 0·861i	7·41
0·14	0·3529 − 0·1120i	−0·242 + 0·863i	7·70
0·16	0·3897 − 0·1064i	−0·258 + 0·866i	8·14
0·18	0·4238 − 0·1000i	−0·271 + 0·870i	8·70
0·20	0·4558 − 0·0933i	−0·282 + 0·875i	9·38
0·24	0·5147 − 0·0794i	−0·300 + 0·888i	11·19
0·28	0·5685 − 0·0657i	−0·316 + 0·904i	13·75
0·32	0·6187 − 0·0525i	−0·329 + 0·925i	17·62

4. DISCUSSION

A comparison of the present numerical results ($\sigma=0{\cdot}70$) for F_0 and H_0 indicates agreement with those of Fujii *et al.* [6] and also with the centerline value of Gebhart *et al.* [3]. However, the global value in [3] for the total thermal convection is off by about 2 per cent which is probably due to either the mesh size being too large or, more likely, to η_e (the value of η out to which the numerical integration is carried) being too small. In particular, the results in [6], accurate to five places, were obtained with a mesh size of $\Delta\eta\simeq0{\cdot}0093$ (in present notation) and $\eta_e\simeq27$. In contrast, the present numerical results were obtained by numerically integrating in from η_e to $\eta=0$, making use of the asymptotic behavior of F_0 and H_0 for large η. This is a standard procedure which has been described recently in the appendix of [7]. In particular, five-place accuracy was obtained by this latter method with $\Delta\eta=0{\cdot}05$ and $\eta_e=8$.

By truncating the series in (3.4) to two terms, it follows that the neutral-stability curve ($\alpha_i\equiv0$) is given by

$$G=-\alpha_{2i}(\Omega)/\alpha_{1i}(\Omega) \tag{4.1}$$

where the RHS has been tabulated in the last column of Table 1. The resulting curve is shown in Fig. 1 together with contours of constant negative values of α_i.

For comparison, the neutral-stability curve of Haaland and Sparrow [7] has also been shown (dashed) in Fig. 1. This latter result is based upon an extension of the coupled Orr–Sommerfeld equations to include the effects of $\tilde{v}_0\partial\tilde{\zeta}/\partial y$ and $\tilde{u}\partial\tilde{\zeta}_0/\partial x$ in the disturbance vorticity equation (and analogous terms in the energy equation). However, as shown by the present analysis, the terms $\tilde{u}_1\partial\tilde{\zeta}/\partial x$ and $\tilde{v}\partial\tilde{\zeta}_1/\partial y$ are also of the same order-of-magnitude, as are effects arising from the algebraic x-dependence in $\tilde{\zeta}$ and the x-dependence of

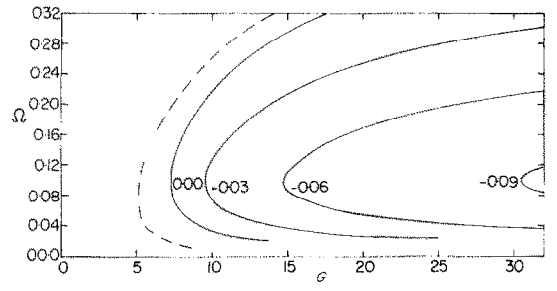

FIG. 1. Contours of constant values of α_i vs G and Ω (for $\sigma = 0{\cdot}70$). Dashed curve is neutral-stability contour of Haaland and Sparrow [7].

α (for fixed physical frequency). Further discussion of the numerical aspects of the stability analysis are given in Appendix A, to which the interested reader is referred.

Since the "critical" value of G in Fig. 1 is seen to be $\approx 7{\cdot}3$, it is to be suspected that effects arising from the $O(\varepsilon^{5/3})$ terms in (2.1)–(2.2) may also be non-negligible in this region of the stability plane. Although the inclusion of these effects would complicate matters unduly, it should be noted that b_1 is a function of the heat-source Grashof number [$Gr \equiv g\beta(T_w - T_\infty)\, a^3/\nu^2$, a being the radius of source] and that (see Appendix B) $b_1 = 0(1)$ as $Gr \to 0$ and $b_1 = O(Gr^{5/12})$ as $Gr \to \infty$. Hence, as Gr increases, the effect of the $O(\varepsilon^{5/3})$ terms extends to larger x/λ and therefore can be expected to have an increased influence upon stability.

Unfortunately, a comparison of the present theory with existing experimental results proves to be indecisive. Some of the major points to be noted in this regard are indicated below.

The experimental results of Brodowicz and Kierkus [1], Forstrom and Sparrow [2] and Schorr and Gebhart [4] show that the centerline temperature does vary as $x^{-3/5}$, in agreement with the zeroth-order plumè theory, but that the magnitude of the temperature is systematically about 15 per cent below the predicted value. Although the negative value of $H_1(0)$ in (2.8) indicates a correction in the right direction, this effect should become negligible with increasing x/λ, which is not borne out by the data.

Perhaps the most characteristic property of the experimental investigations is a slow meandering motion. In fact, despite attempts in [2] at eliminating this effect by isolating the system, the effect was still evident. Unfortunately, as has been suggested by Fujii *et al.* [6], the linear stability theory does not describe this meandering, the observed frequencies being much smaller than theory would indicate. For example, the periodic temperature variations shown in the upper graph of Fig. 5 in [2] correspond to $G \simeq 10$ and $\Omega \simeq 1{\cdot}4 \times 10^{-3}$ whereas, according to Fig. 1 of the present paper, one would expect Ω to be larger by a factor of almost 100. This inadequacy of the stability theory suggests the presence of an additional effect which has not been accounted for. In particular, the fact that the meandering has been observed at such small G suggests that the triggering mechanism may actually occur in the vicinity of the wire. On the other hand, it should be noted that the introduction of controlled oscillations by Pera and Gebhart [5] has shown that the linear stability theory does indeed describe the response of the plume to disturbances in the frequency range of $O(U/\delta)$.

The concept of a virtual displacement in the location of the line heat source has been considered by Forstrom and Sparrow [2] and by Schorr and Gebhart [4]. In both investigations, the virtual-source location was determined experimentally by a method which implicitly assumes that the displacement effect is the only correction to the zeroth-order flow. According to the present analysis, however, the leading correction (F_1 and H_1) is due to the interaction between the plume and the external irrotational flow region, the virtual-source effect first appearing in the terms of $O(\varepsilon^{5/3})$ in (2.1)–(2.2). The relationship of b_1 to the virtual displacement can be demonstrated by merely replacing "x" by "$x - x_0$" in the quantities $U\delta F_0(\eta)$ and $\Delta T H_0(\eta)$ and expanding these expressions for small values of x_0/x (noting the explicit x-dependence of U, δ, η and ΔT); the first two terms in the resulting expansions correspond to the first and third terms in (2.1)–(2.2) provided x_0/λ is replaced by b_1. That is, $b_1\lambda$ can be interpreted as the virtual location of the line source along the x axis. Hence, from the definition of λ and the results in Appendix B, it follows that x_0 is proportional to $Q^{-1/3}$ and independent of a if $Gr \ll 1$ but is linearly proportional to a and independent of Q if $Gr \gg 1$. In order to determine b_1 or x_0 exactly, however, it would be required to determine the flow in the vicinity of the wire; short of that, it appears that the only means of obtaining b_1 would be by an experimental determination of the x-dependence of the centerline velocity or temperature in the region where the higher-order corrections in (2.1) or (2.2) should be discernible (i.e. $\varepsilon \gtrsim 0{\cdot}1$ or, equivalently, $G \lesssim 10$). Based upon the difficulties encountered in the experimental investigations to date, the possibility of obtaining such accurate measurements seems rather remote.

Finally, the results of the present stability theory have been shown in Fig. 2 in terms of contours of constant amplification, where the latter is based upon the exponential growth in the amplitude of a fixed-frequency disturbance as it crosses the neutral curve

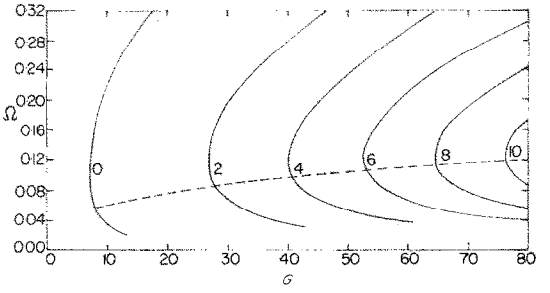

FIG. 2. Contours of constant values of $\exp(-\frac{5}{3}\int \alpha_i dG)$. Dashed curve is trajectory of a constant-frequency disturbance ($\sigma = 0{\cdot}70$).

and propagates downstream:

$$A = \exp\left(-\int_{x_n}^{x} \alpha_i \frac{dx}{\delta}\right) = \exp\left(-\tfrac{5}{3}\int_{G_n}^{G} \alpha_i dG\right),$$

subscript n denoting values along the neutral curve. The path of any such disturbance in the stability plane is given by

$$\Omega = BG^{1/3}$$

where B is a numerical constant; in particular, the path shown (dashed) in Fig. 2 corresponds to $B = 0{\cdot}028$ which, based upon the property values of air, reduces to

$$\omega \simeq \left(\frac{1{\cdot}22}{\text{s}}\right)\left(\frac{Q}{\text{W/m}}\right)^{2/3}.$$

A typical end result of linear-stability analyses is the establishment of an empirically based correlation between the observed transition-to-turbulence and a particular value of A_{max}. That is, for given classes of flow it has been found that the "point" of turbulent transition occurs at the value of $U\delta/\nu$ ($\equiv G$, in the present case) for which A_{max} has a certain value—e^9 for forced-flow boundary layers [11], e^{10} for natural-convection boundary layers along vertical surfaces [12]. Although the establishment of such a correlation for the present case is precluded by a paucity of transition data, it might be noted that Forstrom and Sparrow [2] identified the first appearance of turbulent bursts with $G \approx 50$ (which, from Fig. 2, corresponds to $A_{max} \approx e^6$) and the establishment of "fully" turbulent flow with $G \approx 80$ (corresponding to $A_{max} \approx e^{10}$).

REFERENCES

1. K. Brodowicz and W. T. Kierkus, Experimental investigation of laminar free-convection flow in air above horizontal wire with constant heat flux, *Int. J. Heat Mass Transfer* **9**, 81–94 (1966).
2. R. J. Forstrom and E. M. Sparrow, Experiments on the buoyant plume above a heated horizontal wire, *Int. J. Heat Mass Transfer* **10**, 321–331 (1967).
3. B. Gebhart, L. Pera and A. W. Schorr, Steady laminar natural convection plumes above a horizontal line heat source, *Int. J. Heat Mass Transfer* **13**, 161–171 (1970).
4. A. W. Schorr and B. Gebhart, An experimental investigation of natural convection wakes above a line heat source, *Int. J. Heat Mass Transfer* **13**, 557–571 (1970).
5. L. Pera and B. Gebhart, On the stability of laminar plumes: some numerical solutions and experiments, *Int. J. Heat Mass Transfer* **14**, 975–984 (1971).
6. T. Fujii, I. Morioka and H. Uehara, Buoyant plume above a horizontal line heat source, *Int. J. Heat Mass Transfer* **16**, 755–768 (1973).
7. S. E. Haaland and E. M. Sparrow, Stability of buoyant boundary layers and plumes, taking account of non-parallelism of the basic flows, *J. Heat Transfer* **95C**, 295–301 (1973).
8. C. A. Hieber, Natural convection around a semi-infinite vertical plate: higher-order effects, *Int. J. Heat Mass Transfer* **17**, 785–791 (1974).
9. K. Stewartson, *The Theory of Laminar Boundary Layers in Compressible Fluids*, Section 3.5. Oxford University Press, Oxford (1964).
10. C. C. Lin, *The Theory of Hydrodynamic Stability*. Cambridge University Press, Cambridge (1966).
11. A. M. O. Smith, Transition pressure gradient and stability theory, *Proc. 9th Int. Congr. of Appl. Mech., Brussels*, Vol. 4, pp. 234–244 (1957).
12. C. A. Hieber and B. Gebhart, Stability of vertical natural convection boundary layers: some numerical solutions, *J. Fluid Mech.* **48**, 625–646 (1971).
13. R. E. Kaplan, The stability of laminar incompressible boundary layers in the presence of compliant boundaries, Mass. Inst. Tech., Aeroelastic and Structures Research Lab. TR 116-1 (1964).
14. J. J. Mahony, Heat transfer at small Grashof number, *Proc. R. Soc.* **A238**, 412–423 (1957).

APPENDIX A

Some Numerical Aspects of the Stability Analysis

It is noted that the asymptotic behavior of ϕ_1 and ϕ_2 for large η is given by

$$\phi_1 \sim e^{-\alpha_1\eta} \tag{A1}$$

and

$$\phi_2 \sim (\beta_0 + \beta_1\eta + \beta_2\eta^2)e^{-\alpha_1\eta} \tag{A2}$$

where β_1 and β_2, arising from the limiting behavior of the inhomogeneous terms in (3.14), are given by

$$\beta_2 = \frac{i\alpha_1}{5}, \quad \beta_1 = \frac{(\frac{4}{5}i\alpha_1 + \frac{1}{5}i\gamma + 2\beta_2 - 2\alpha_1\alpha_2)}{2\alpha_1} \tag{A3}$$

and where $\beta_0 \equiv 0$ (i.e. the disturbance field has been normalized by defining the coefficient of the $e^{-\alpha_1\eta}$ term in ϕ to be identically one). A plot of the absolute value of ϕ_1', ϕ_2', $-i\alpha_1\phi_1$ and $(\frac{2}{5}\eta\phi_1' - \frac{3}{5}\phi_1 - i\alpha_2\phi_1 - i\alpha_1\phi_2)$ vs η is shown in Fig. 3 for $\Omega = 0{\cdot}10$. In particular, the peaks exhibited by the second-order terms are associated with the "critical layer", i.e. the region in the vicinity of the point where $F_0'(\eta) = c_1$ (in the complex η-plane); e.g. for the case of $\Omega = 0{\cdot}10$, $c_1 = \Omega/\alpha_1 \simeq 0{\cdot}312 + 0{\cdot}137i$ whereas $F_0'(\eta) = 0{\cdot}312$ at $\eta \simeq 2{\cdot}73$. Based upon similar print-outs at $\Omega = 0{\cdot}04$ and $0{\cdot}20$, it is noted that, with increasing Ω, the peak in the second-order terms becomes larger and moves towards the centerline while the first-order terms actually diminish in magnitude (in the framework of the above normalization).

For comparison, it is noted that the previous stability analyses of the plume, [5] and [7], have represented the disturbance field by

$$\left.\begin{aligned} \phi &= \Phi_1 + B_2\Phi_2 + B_3\Phi_3 \\ 0 &= \Theta_1 + B_2\Theta_2 + B_3\Theta_3 \end{aligned}\right\} \tag{A4}$$

where each (Φ_j, Θ_j) is an integral of the coupled Orr–Sommerfeld equations (of "extended" form, in [7]), $j = 1$ corresponding to the inviscid limit and $j = 2, 3$ being characterized by viscous effects. However, as pointed out by Lin [10], in such cases as the plume in which no solid walls are present, B_2 and B_3 must be identically zero since Φ_2 and Φ_3 are such that if they vanish as $\eta \to \infty$ then they are unbounded as $\eta \to -\infty$. That B_2 and B_3 were found to be non-zero in [5] and [7] is attributed to the fact that the numerical procedure of determining Φ_1 from the full Orr–Sommerfeld equations introduces multiples of Φ_2 and Φ_3. Hence, unless a purification scheme such as that of Kaplan [13] is employed, B_2 and B_3 will have to be non-zero in order to cancel the spurious Φ_2 and Φ_3 behavior in the numerically determined Φ_1. The point to be noted then is that Φ_2 and Φ_3 are, in fact, not present in the plume case and that, in leading approximation (i.e. for large G, as has been assumed throughout), the disturbance field is characterized by the inviscid equation, (3.13). Seen in this light, the "bottling" concept in [7] seems somewhat ill-founded although it is interesting to note that, based upon (A1) and (A2), the asymptotic behavior of the $O(U/(\varepsilon x))$ and $O(U/x)$ terms in (3.10) vanish identically, indicating that the disturbance vorticity does indeed decay more rapidly than that of the base flow. On the other hand, it is seen from Fig. 3 that the disturbance velocity decays slowly howbeit more rapidly than the base-flow velocity since the latter approaches non-zero values as it merges with the irrotational flow outside.

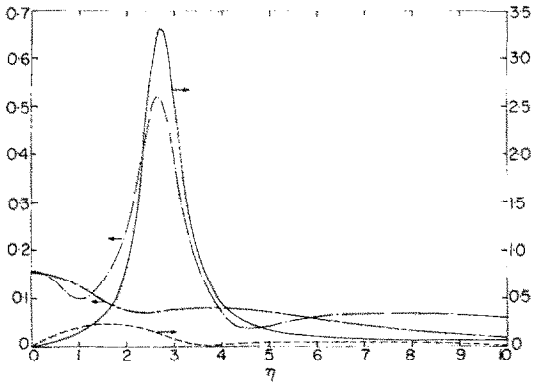

FIG. 3. Profiles at $\Omega = 0{\cdot}10$ of the following disturbance quantities: $|\phi_1'|$, ----, $|\phi_2'|$, ———; $|-i\alpha_1\phi_1|$, — — —; $|\frac{3}{5}\eta\phi_1' - \frac{3}{5}\phi_1 - i\alpha_2\phi_1 - i\alpha_1\phi_2|$, —·—· ($\sigma = 0{\cdot}70$).

In passing, it might be noted that a stability analysis similar to the present one can presumably also be applied e.g. to the natural-convection boundary layer on a vertical plate. In that case, Φ_2 and Φ_3 will be required in order to satisfy the non-slip and thermal condition at the wall. However, as indicated in [12], the effects of $(\ )_2$ and $(\ )_3$ will be confined to the region $\eta = O(G^{-1/2})$. Hence, although the limiting equations in the region $\eta = O(1)$ will be the same as in the present case, the boundary conditions at $\eta = 0$ will be replaced by matching conditions with a predominantly viscous inner layer.

APPENDIX B

Behavior of b_1 *for Limiting Values of* Gr

(i) $Gr \ll 1$

This limiting case was analyzed and solved approximately in the classic paper by Mahony [14]. An exact solution to the flow around the cylinder would require solving the full governing equations (subject to the Boussinesq approximation) in the outer region. To the authors' knowledge, this has not been done yet although it may now be within the capability of present-day computers. The following qualitative treatment is based upon matched-asymptotic-expansion considerations.

In the region $r = O(a)$, the temperature field is conduction-dominated with

$$T \sim T_w - O(\varepsilon_1 \overline{\Delta T}), \quad \varepsilon_1 \equiv \frac{1}{\log \frac{1}{Gr}} \tag{B1}$$

where $\overline{\Delta T} \equiv T_w - T_\infty$. In the "outer" region, where

$$r = O\left(\frac{a}{\varepsilon_2}\right), \quad \varepsilon_2 \equiv \left(\frac{Gr}{\log \frac{1}{Gr}}\right)^{1/3}, \tag{B2}$$

thermal convection and conduction are of the same order-of-magnitude with inertial, viscous and buoyant effects being comparable in the momentum equation. This results in

$$T \sim T_\infty + O(\varepsilon_1 \overline{\Delta T}), \quad |\mathbf{v}| = O\left(\varepsilon_2 \frac{\nu}{a}\right). \tag{B3}$$

Beyond the outer region, i.e. for $r > O(a/\varepsilon_2)$, the flow is characterized by an irrotational flow within which is embedded a thin rotational region along the vertical axis (the plume).

In order to show that the plume structure of Section 2 merges with the outer region, it must first be noted that (B1) implies

$$Q = O(\varepsilon_1 k \overline{\Delta T}). \tag{B4}$$

Hence,

$$\tilde{\Delta T} \equiv \frac{Q}{k} = O(\varepsilon_1 \overline{\Delta T}) \tag{B5}$$

and

$$\lambda \equiv \left(\frac{\nu^2}{g\beta \tilde{\Delta T}}\right)^{1/3} = O\left(\frac{a}{\varepsilon_2}\right). \tag{B6}$$

Therefore,

$$U \equiv \frac{\nu}{\lambda}\left(\frac{x}{\lambda}\right)^{1/5} = O\left\{\varepsilon_2 \frac{\nu}{a}\left(\frac{x}{\lambda}\right)^{1/5}\right\} \tag{B7}$$

and

$$\Delta T \equiv \tilde{\Delta T}\left(\frac{\lambda}{x}\right)^{3/5} = O\left\{\varepsilon_1 \overline{\Delta T}\left(\frac{\lambda}{x}\right)^{3/5}\right\} \tag{B8}$$

from which it follows that $U = O(\varepsilon_2 \nu/a)$ and $\Delta T = O(\varepsilon_1 \overline{\Delta T})$ if $x = O(\lambda) = O(a/\varepsilon_2)$. That is, the plume structure does merge with the outer region described by (B2) and (B3).

Since the indeterminacy in (2.1)–(2.2) arises from the flow behavior in the vicinity of the heat source, it follows that $b_1 \varepsilon^{5/3}$ should become of $O(1)$ as the outer region is approached from the plume region, i.e. as x decreases to $O(a/\varepsilon_2)$. But if $x = O(a/\varepsilon_2)$ then $\varepsilon = O(1)$, implying that $b_1 = O(1)$.

(ii) $Gr \gg 1$

In this limit, it is well known that the flow in the vicinity of the cylinder is characterized by a boundary layer, of $O(\delta_1)$ in thickness, where

$$\delta_1 \equiv \frac{a}{Gr^{1/4}}, \quad |\mathbf{v}| = O\left(\frac{\nu}{a} Gr^{1/2}\right). \tag{B9}$$

From δ_1 it then follows that

$$Q = O(k\overline{\Delta T} Gr^{1/4}). \tag{B10}$$

Hence,

$$\tilde{\Delta T} = O(\overline{\Delta T} Gr^{1/4}), \quad \lambda = O\left(\frac{a}{Gr^{5/12}}\right) \tag{B11}$$

from which it follows that

$$U = O\left\{\frac{\nu}{a} Gr^{5/12}\left(\frac{x}{\lambda}\right)^{1/5}\right\}, \quad \Delta T = O\left\{\overline{\Delta T} Gr^{1/4}\left(\frac{\lambda}{x}\right)^{3/5}\right\}. \tag{B12}$$

Therefore, when $x = O(a)$, it follows from (B11) and (B12) that

$$U = O\left(\frac{\nu}{a} Gr^{1/2}\right), \quad \Delta T = O(\overline{\Delta T}) \tag{B13}$$

which is seen to agree with the behavior in the boundary layer surrounding the cylinder.

In this case, we expect $b_1 \varepsilon^{5/3}$ to be $O(1)$ where $x = O(a)$, hence $\varepsilon^{5/3} = \lambda/x = O(Gr^{-5/12})$. Therefore, $b_1 = O(Gr^{5/12})$.

CONVECTION NATURELLE AU DESSUS D'UNE SOURCE LINEIQUE DE CHALEUR: EFFETS D'ORDRE SUPERIEUR ET STABILITE

Résumé—Le sillage de convection naturelle au dessus d'une source linéique horizontale de chaleur est étudié à l'aide de la théorie de la couche limite à un ordre d'approximation supérieur. Une étude de stabilité de l'écoulement de base obtenu est effectuée à l'aide d'un développement systématique du champ de perturbation. La comparaison de la théorie avec les résultats expérimentaux existants est peu concluante.

DIE NATÜRLICHE KONVEKTION ÜBER EINER LINIENFÖRMIGEN WÄRMEQUELLE: AUSWIRKUNGEN HÖHERER ORDNUNG UND STABILITÄT

Zusammenfassung—Die freie Konvektionsströmung über einer horizontalen, linienförmigen Wärmequelle wird nach Gliedern höherer Ordnung der Grenzschichttheorie untersucht. Eine Stabilitätsanalyse mittels einer systematischen Erweiterung für das Störfeld wird dann für die resultierende Grundströmung durchgeführt. Ein Vergleich der Theorie mit den vorhandenen experimentellen Ergebnissen ist nicht beweiskräftig.

ЕСТЕСТВЕННАЯ КОНВЕКЦИЯ НАД ЛИНЕЙНЫМ ИСТОЧНИКОМ ТЕПЛА: ЭФФЕКТЫ ВЫСШЕГО ПОРЯДКА И УСТОЙЧИВОСТЬ

Аннотация — Анализируется естественная конвекция над горизонтальным линейным источником тепла в членах высшего порядка теории пограничного слоя. Затем, с помощью систематического разложения поля возмущений проводится анализ устойчивости основного течения. Проведенное сравнение теоретических данных с имеющимися экспериментальными результатами не является доказательным.